

Integrated Geophysical Methods Approach to Mineral Exploration in the Wadi Araba Area, Southern Jordan

¹Abdallah S. Al-Zoubi, ¹Awni T. Batayneh and ²Ziad S. Abu-Hamattah

¹Research and Studies Department, Faculty of Graduate Studies and Scientific Research
Al-Balqa' Applied University, Al-Salt 19117, Jordan

²Natural Resources and Chemical Engineering Department, Tafila Applied University Collage
Tafila P. O. Box 26, Tafila 66141, Jordan

Abstract: Detailed geophysical investigation was conducted in the east central part of Wadi Araba area utilizing Horizontal-Loop Electromagnetic (HLEM), magnetic, gravity and induced polarization to investigate the subsurface geological features and the possible mineralization zones. The results of potential field methods outline intense positive and negative anomalies trending NW-SE. This feature is either a dyke, or a fault-bounded block of different rock types. The electromagnetic survey reveals significantly altered zones (conductive bodies) trending NNW-SSE and NW directions. The Induced Polarization surveys were presented in pseudo-sections representing the apparent resistivity and metal factors. The alteration zone probably indicates presence of mineralization along the NNW-SSE contact between the basement complex (Precambrian) and the overlying younger sedimentary rocks.

Key Words: Geophysical Methods, Mineral Exploration, Wadi Araba Area, Jordan

Introduction

Geophysical techniques proved to be an effective tool in locating and detecting different features such as faults, alteration zones and dykes. The geophysical surveys carried out in the east central part of Wadi Araba were aimed to:

1. evaluate the resolution of geophysical techniques in field work in detecting and locating anomalies of vein like bodies and
2. examine the capability of geophysical survey and it's results in detecting targets in order to implement in other locations.

Prompted largely by this interest, Horizontal-Loop Electromagnetic, induced polarization, magnetic and gravity geophysical surveys were undertaken to provide information on the configuration and variations of the Precambrian rocks, the thickness and, possibly, the structure of the overlying sedimentary rocks. An essential part of the Horizontal-Loop Electromagnetic (HLEM), Induced Polarization (IP), magnetic and gravity geophysical surveys interpretation was incorporated with available geological data to produce a final geological meaningful interpretation. It was hoped that the results would illustrate the usefulness of detailed electromagnetic, induced polarization, magnetic and gravity interpretation in solving the ambiguities of the structural geology and tectonics of the study area.

The study area lies in the western part of the Arabian Platform and within Wadi Araba-Dead Sea-Jordan Transform Fault, which extends from the northern part of the Red Sea (Gulf of Aqaba) up to East Anatolian fault (Fig. 1), with about 105 km of left-lateral strike slip displacement. The nature of this transform fault is related to the opening of the Red Sea (Quennell, 1958; Mart and Hall, 1984; Mart and David, 1987). According to Frei and Freund (1990), the opening of the Red Sea took place in two stages: (a) Late-Early Oligocene and (b) from about 5 million onward. The northern Red Sea is characterized by its bifurcation into the Gulf of Suez and Gulf of Aqaba (Fig. 1). In terms of plate tectonics, the Red Sea opening is transformed and directly linked to the opening and

extension of the Gulf of Aqaba-Wadi Araba-Dead Sea rift (Fig.1).

Geological Setting: The study area lies in the east central part of Wadi Araba, about 93 km north of the Gulf of Aqaba (Fig. 1). The study area incorporates Late Proterozoic and Early Cambrian Aqaba and Araba Complexes, Safi Group and Ahaymir volcanic. The first two complexes are calc-alkaline granitoids and alkaline magmatic activity which is part of the Arabian-Nubian Shield, whereas the Safi Group represents an episode of erosion and deposition of fluvial sediments mainly of igneous origin, where is the Ahaymir volcanics are predominantly rhyolites (Rabba *et al.*, 1999).

The Geological map (Fig. 2) of the study area shows the following units:

1. The Hawar Two-Mica Granite (HR) is exposed in the southern and central part of the study area (Fig. 2) and contains equal amounts of biotite and muscovite in parallel bands, veins and dykes of simple pegmatite's comprises mainly of muscovite, quartz, orthoclase, that are dominant in the syenogranite-monzogranite of the Hawar Two-Mica granite.
2. The Hayyala Vocaniclastic Formation (HV) of the Safi Group is partly younger than the Aqaba Complex and consists of sub-rounded clasts of rhyolites, mud, pebbles and cobbles in green-gray arkosic matrix that overlain by well bedded coarse tuff and varied mudstone and siltstone, green weathering tuffs and ignimbrites. The formation is exposed in the eastern part of the study area (Fig. 2) and around the crushed zone.
3. The Qusayb Rhyolite Unit (QB) consists of massive, fine-grained porphyritic and non-porphyritic flow-banded rhyolitic lava and rare copper mineralization. Phenocrysts comprise subhedral to idiomorphic vitreous quartz and red-pink feldspar, set in an orange-brown aphanitic matrix.
4. The Musaymir Rhyolite Unit (MR) consists of porphyritic rhyolites. It exhibits flow structure and includes parallel devitrified glass shards with angular dark brown rhyolite fragments.

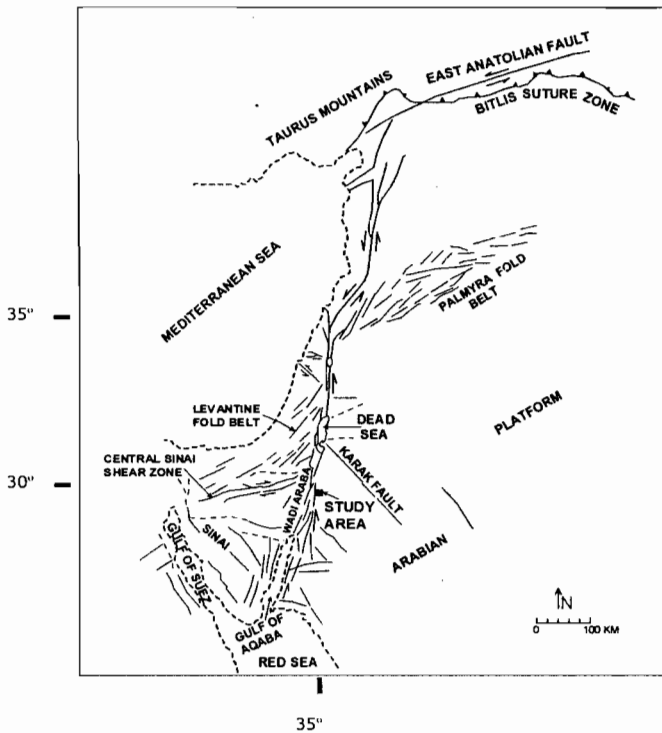


Fig. 1: Generalized Tectonic Map of the Dead Sea Transform Fault (Modified From Barazangi, 1983)

5. The Xenolithic Agglomerate Unit (XG) can be subdivided into two different lithological members: The green xenolithic agglomerate is bedded in many localities with intrusive granite, schist, gneissic xenoliths of variable size (0.1 up to 3 m diameter) and the red xenolithic agglomerate is similar to the green unit, but different in the color and low content of xenoliths. The tuff Unit is characterized by thin and thick beds of green tuff, in general, with no xenoliths and overlies the xenolithic agglomerate unit in many places.
6. The Mofarqida Conglomerate Unit (MC) consists of polymict conglomerate comprising angular to sub-angular clasts-supported, poorly sorted cobbles and boulders.

One of the most significant geological features of the basement rocks is the abundance of dykes that cut across the studied granitoids and volcanic units in the study area. They can be broadly subdivided into two major types: rhyolite porphyry, which is the dominant, and the dolerite. The concentration of dykes in the plutonic crystalline rocks is more than the volcanic acidic rocks. Unique bearing Au-dyke which crosses the volcanic acidic units, trending NW-SE (Warwick *et al.*, 1996), is present in the central northern part of the study areas (Fig. 2).

The sedimentary rock record in the study area (Fig. 2) incorporates mainly Cambrian, Cretaceous and Quaternary sediments. These are in ascending order, Salib Arkosic Sandstone Formation (SB), Abu-Khusheiba Sandstone Formation (AK) and Umm Ishrin Sandstone Formation (IN), Cretaceous and superficial sediments. The Paleozoic rocks in the study area show

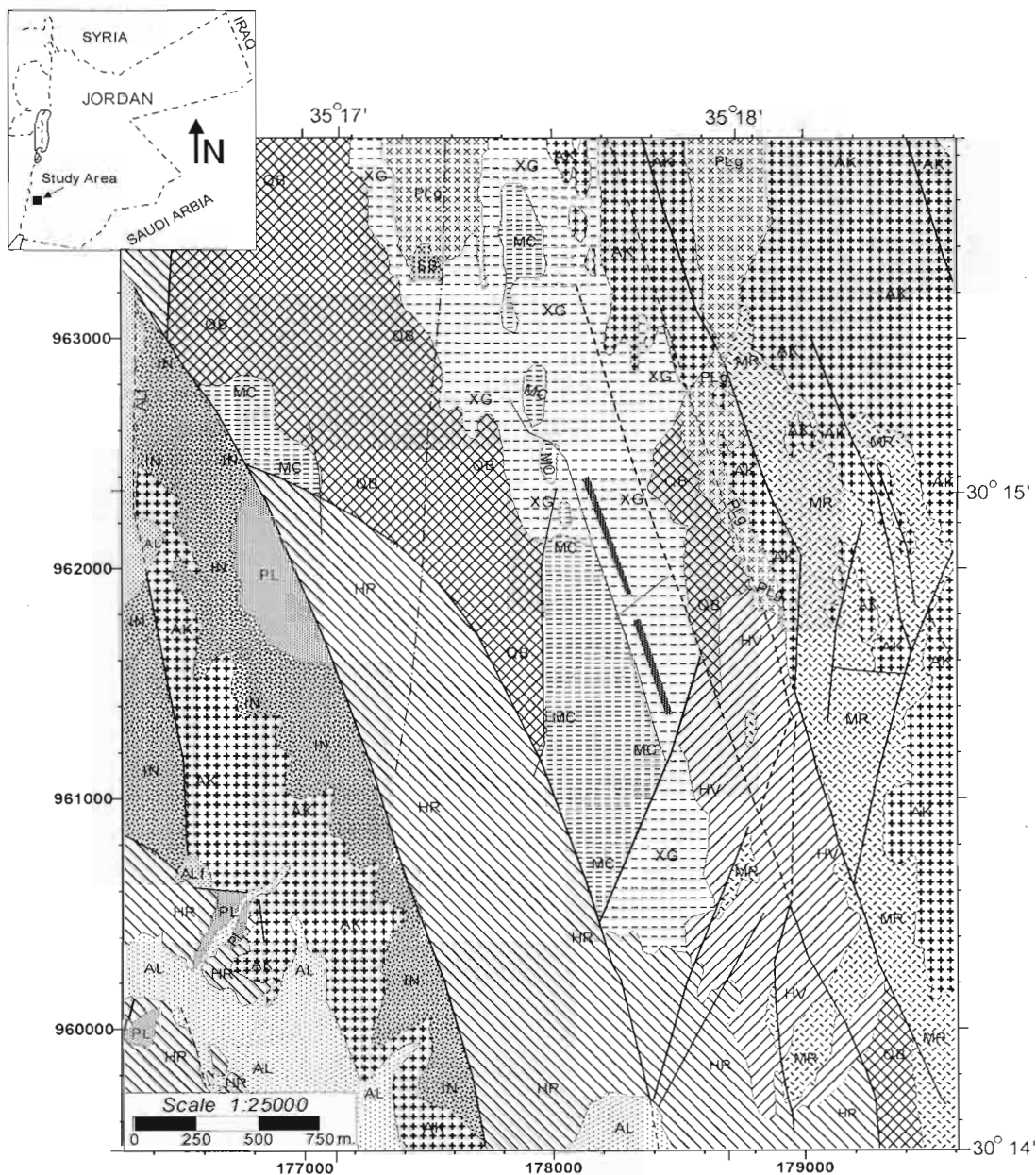
a regional dips towards northeast (Rabba *et al.*, 1999). The Salib Arkosic Sandstone Formation (Early Cambrian) forms the lower most part of the Rain Sandstone Group (Cambrian-Ordovician) and unconformably overlies either the irregular erosion surface developed on the Aqaba and Araba granitoids or on the immature palaeotopography of the Ahaymir volcanic rocks. The formation ranges in thickness from 0-60 m and has a restricted distribution in the study area. It is mainly exposed in the southeastern part of the area. The depositional environment was dominantly continental alluvial braided plain (Rabba *et al.*, 1999). The Abu Khusheiba Sandstone Formation (Late to Middle Cambrian) overlies either the Salib Arkosic Sandstone or onlaps the palaeohigh of the basement igneous rocks. This formation is 0-110 m thick and has a broad distribution in the study area. It is mainly exposed in the north eastern and central western parts of the area in a half-graben system. The regional dip of the strata is 20°- 40° to the NE. Generally, the formation consists of white to pale gray and pinkish red, fine-to medium-grained, micaceous sandstone and siltstone that contain fragments of rhyolite (locally derived from Ahaymir volcanic). The depositional environment was transitional between the fully marine and the fluvial sediments. Copper mineralization occurs in several horizons within this formation (Rabba *et al.*, 1999).

The Umm Ishrin Sandstone Formation (Middle-Late Cambrian) overlies the Abu Khusheiba Sandstone Formation and crops out in the northeastern and central western parts of the study area in a down faulted blocks (half graben). In the frame of this study, no complete section of this formation has been recorded. In the meantime the formation is up to 300m thick. The strata of this formation are dipping 30° to the NE. Generally, the formation consists of red brown to yellow-brown and mauve-red, medium to coarse-grained massive sandstone. Lenses of white massive sandstone occur within the upper most part of this formation. Colour banding which is the most characteristic feature of this formation exposed locally in the southern part of the area. The depositional environment was continental fluvial braided stream with a few marine incursions (Rabba *et al.*, 1999).

Cretaceous rocks are exposed in the extreme northwestern part of the area; in a highly tectonic controlled area and includes in ascending order; Kurnub Sandstone Group, Na'ur Limestone Formation, Fuhays/Hummar/Shu'ayb formations and Amman Silicified Limestone Formation.

The Kurnub Sandstone Group (Aptain to Early Cenomanian) is up to 160 m thick in the surrounding areas. Generally, the group consists of gray, pale yellow and pink, coarse grained sandstone with scattered quartz pebbles on the surface of the sediments and on the troughs of the forest (Rabba *et al.*, 1999).

The Na'ur Limestone Formation (Cenomanian) overlies the Kurnub Sandstone Group unconformably and consists of massive carbonate units, nodular, light gray and brown dolomitic limestone. The formation is 25-60 m thick in the region. The strata of this formation are dipping to the west, northwest and southwest. The depositional environment was shallow marine to fully marine, subtidal (Rabba *et al.*, 1999).



Legend





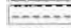


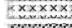



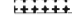
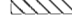
- | | |
|------------------------------------------------------------------------------------------------------------------------|------------------------------------------------------------------------------------------------------------------|
|  Gold Dyk ^e |  Salib Arkosic sandstone (SB) |
|  Alluvium (AL) |  Mofarqida Conglomerate (MC) |
|  Wadi Sediment (ALf) |  Xenolithic Agglomerate (XG) |
|  Fluviatil Gravel (PL) |  Musaymir Effusive (MR) |
|  Pleistocene Fluviatil Gravel (PLg) |  Qusayb Rhyolite (QB) |
|  Umm Ishrin Sandstone (IN) |  Hayyala Vulcaniclastic (HV) |
|  Abu Khushayba Sandstone (AK) |  Hawar Two-Mica Granite (HR) |

Fig. 2: Geological Map of the Study Area (after Rabba *et al.*, 1999)

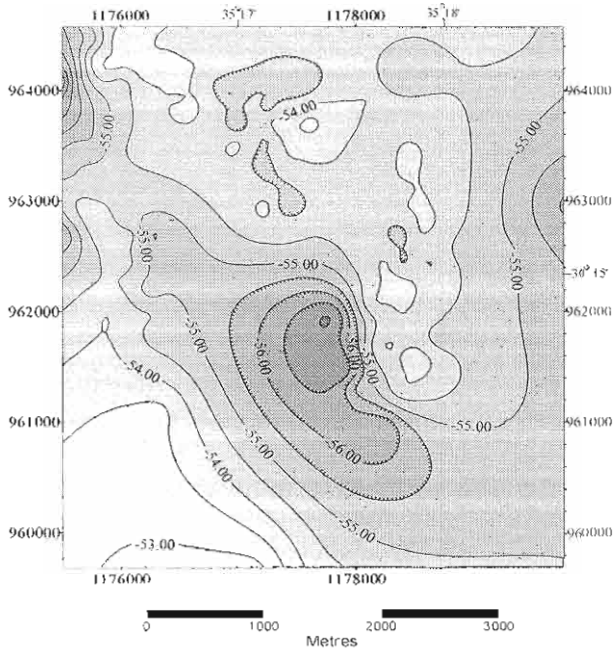


Fig. 3. Bouguer Gravity Map of the Study Area

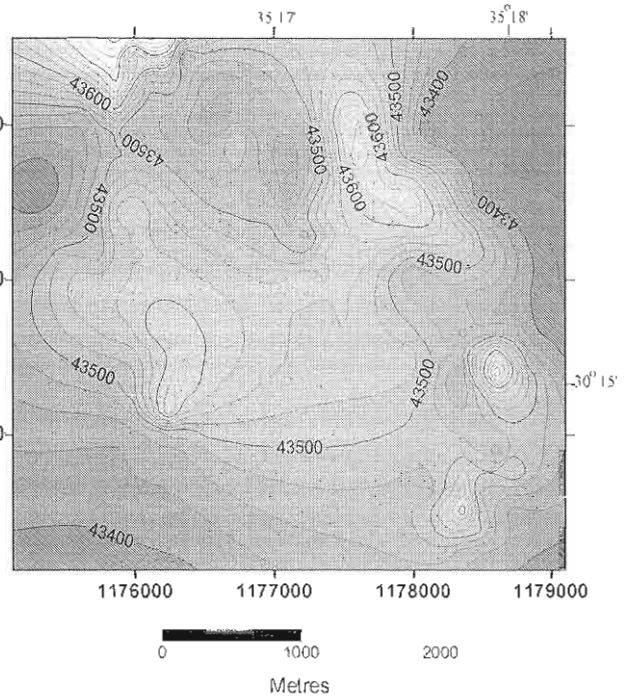


Fig. 4: Magnetic Anomaly Map of the Study Area

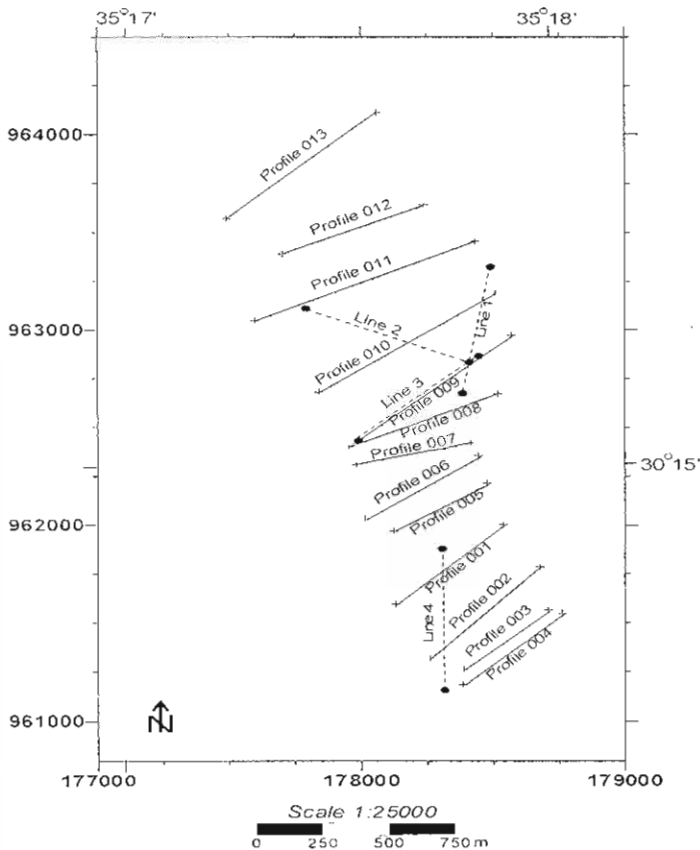


Fig. 5: Site Map Showing EM and IP Profiles. Solid Lines Represent EM Profiles. Dashed Lines Represent IP Profiles

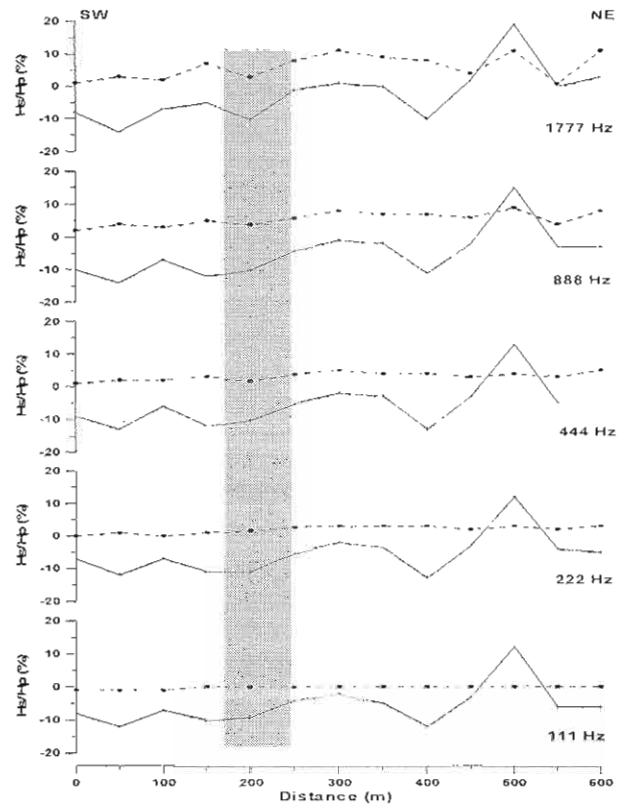


Fig. 6: Horizontal-Loop EM Data along Profile 002 (for Locations Fig. 5) Solid Lines Represent in-Phase Component. Dashed Lines Represent Quadrature Component. Gray Hachure Indicates EM Anomalies

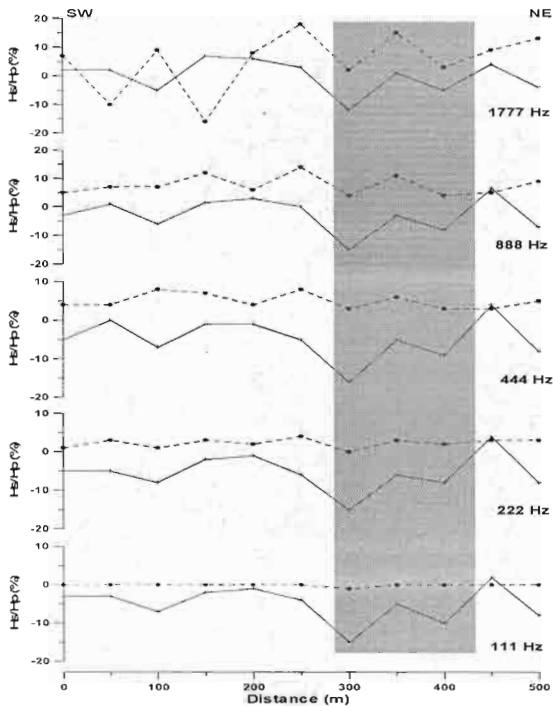


Fig. 7: Horizontal-Loop EM Data along Profile 004 (for Locations Fig. 5). Solid Lines Represent in-Phase Component. Dashed Lines Represent Quadrature Component. Grey Hachure Indicates EM Anomalies

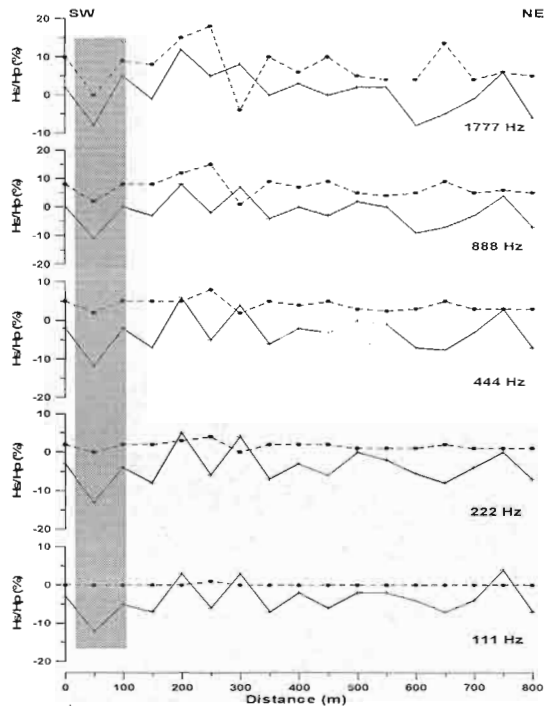


Fig. 9: Horizontal-Loop EM Data along Profile 009 (for Location Fig. 5). Solid Lines Represent in-Phase Component. Dashed Lines Represent Quadrature Component. Gray Hachure Indicates EM Anomalies

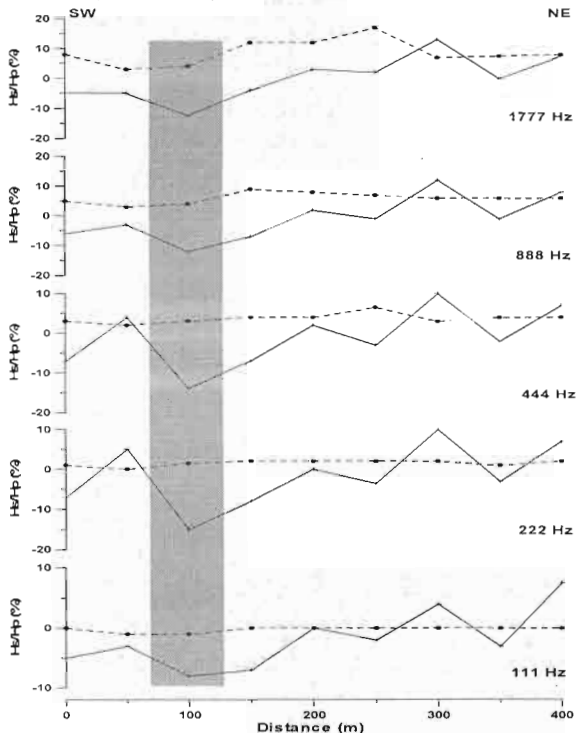


Fig. 8: Horizontal-Loop EM Data along Profile 005 (for Location Fig. 5). Solid Lines Represent in-Phase Component. Dashed Lines Represent Quadrature Component. Grey Hachures Indicate EM Anomalies

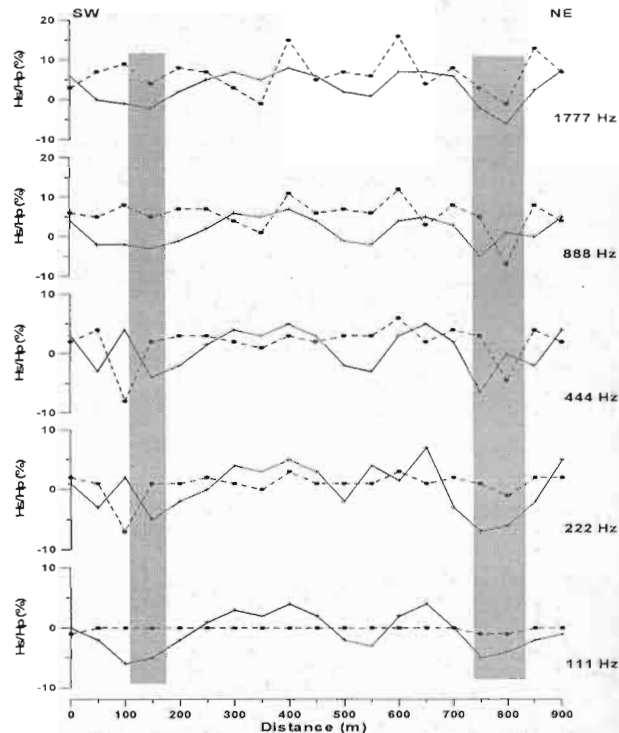


Fig. 10: Horizontal-Loop EM Data along Profile 0011 (for Location Fig. 5). Solid Lines Represent in-Phase Component. Dashed Lines Represent Quadrature Component. Gray Hachures Indicate EM Anomalies

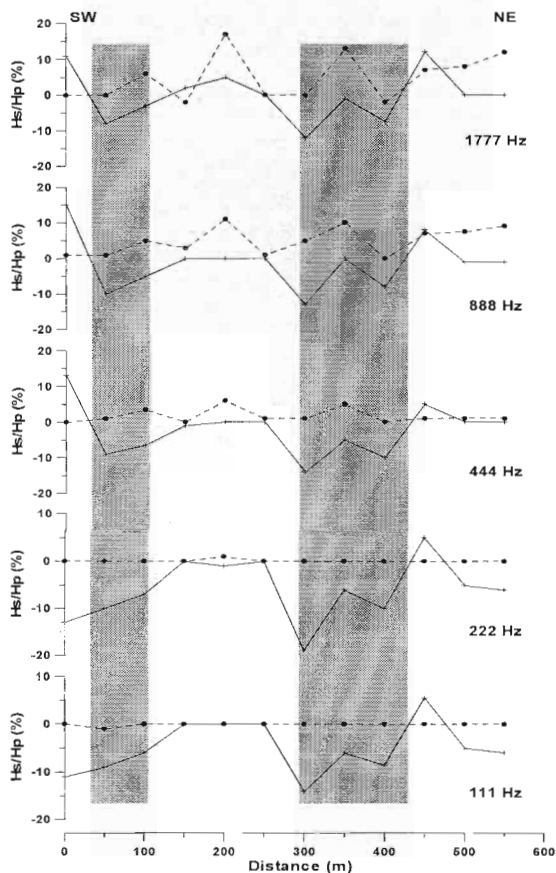


Fig. 11: Horizontal-Loop EM Data along Profile 0012 (for Location Fig. 5). Solid Lines Represent in-Phase Component. Dashed Lines Represent Quadrature Component. Gray Hachures Indicate EM Anomalies

The overlying Fuhays/Hummar/Shu'ayb Formations (undifferentiated) Cenomanian-Lower Turonian, are present locally in the northwestern part of the area. Generally, the Fuhays/Hummar/Shu'ayb Formations ranges between 80-110 m thick and consists of green red pinkish calcareous siltstone, mudstone, gypsum with greenish and reddish mudstone. The depositional environment was open marine to supratidal. The Amman Silicified Limestone Formation (Santonian-Campanian) crops out at one locality, in a graben trending NE-SW in the northwestern part of the area. The exposed thickness of this formation is up to 15 m thick. The strata of this formation are dipping 70° to the SE. The exposed part of this formation consists of chert interbedded with phosphatic chert, limestone, dolomitic limestone concretions and marly limestone. This formation was deposited in a subtidal to shallow continently shelf environment (Rabba *et al.*, 1999). Superficial sediments in the study area include; Pleistocene sediments, alluvium and Wadi sediments, alluvial fans and old alluvial fans and aeolean sand. Pleistocene sediments and old alluvial fans, which represent part of the old drainage system, are present as elevated wadi terraces above the present-day wadi sediments. Unsorted and poorly sorted alluvial sediments occur extensively in the study area. Alluvial

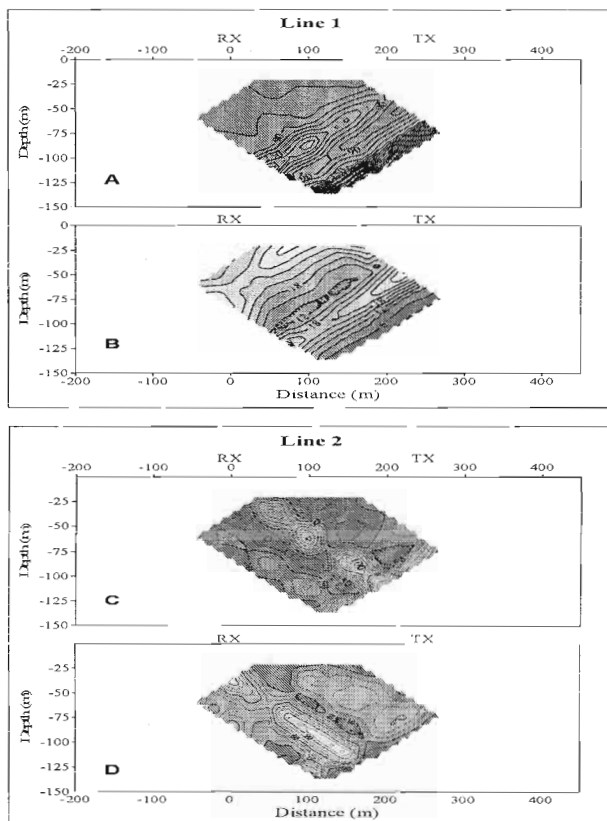


Fig. 12: Pseudo Section of the IP (Time Domain) along the Lines 1 and 2 (for Location Fig. 5). Pseudo Sections (a and c) Represent Apparent Resistivity (P_a). Sections (b and d) Represent Metal Factor (MF)

sediments, which consist of gravel's, sands, silts and fine lose are present on most of hill slops. The present-day wadi sediments consist of unsorted, well-rounded to sub-rounded gravels of variable composition depending on the source area. The active wadi sediments cover the lowest parts of the wadi profiles. Alluvial fans of various size and provenance are developed at different elevations. However, blown sand covers local areas in the northeastern part of the study area (Rabba *et al.*, 1999). Structurally, faulting is the most important structural element that can be observed in the area. The area has been affected by three main fault trends; they are NW-SE, NNW-SSE and NNE-SSE trends. Tectonically, the area had a long tectonic history in different geological eras. NE-SW tensional forces during Late Proterozoic or early Paleozoic have affected the area. Weakness zones of NW-SE trend were created during this tectonic phase, where rhyolite, dolorite dykes were intruded the basement rocks along the weakness zones. The most important tectonic phase is the Late Tertiary phase, where the Arabian Plate is affected by SE-NW compressional stresses that reactivate the weakness zones as normal faults and tilted the blocks to the east forming half graben. This tectonic phase still active, in Quaternary to Recent, as indicated by

the shifting of alluvial fans in Wadi Araba along the Dead Sea transform fault (Bender, 1974 and Rabba et al., 1999).

Geophysical Applications

Gravity Survey: The gravity survey, which was conducted in the eastern side of Wadi Araba (study area), is mainly aimed to detect structures. A total of 249 gravity stations were measured, using the Lacoste and Romberg gravimeter (Model G 880). All observed gravity measurements were tied to one gravity base station. All observed gravity values were calibrated using USGS software package. This software package executes all gravity corrections utilizing two densities 2550 and 2670 kg/m³ to obtain the value of Bouguer gravity anomaly (Fig. 3).

Magnetic Survey: In study area, the ground magnetic measurements were performed using the Proton Magnetometer (Model G856) which measures the total magnetic field with an accuracy of + 1 gamma (nT). A total of 249 magnetic station was measured in the study area. Magnetic data were corrected to a diurnal variation on the basis of reference base station readings and to a common datum. The results of the field measurements were presented as contour map with 20 nT contour interval (Fig. 4).

Horizontal-Loop Electromagnetic (HLEM): HLEM data were acquired using the APEX MAX MIN III equipment that is a multi-frequency induction sensor developed at Parametric Limited, Canada. The APEX MAX MIN III is a horizontal/vertical-loop electromagnetic instrument operating at frequencies 111, 222, 444, 888 and 1777 Hz. The separation intervals of the transmitting and receiving coil vary between 50 and 300 m. The instrument and its uses in mineral prospecting have been described by Betz (1975, 1976). HLEM measurements were acquired along thirteen profiles (L1-L13, Fig. 5) at stations spaced 50 m apart. The location of the survey traverse was marked using GPS positioning (Sokkisha-DT2, Japan). The electromagnetic response was collected at 50 m Tx-Rx separation, at all five transmitter frequencies.

Induced Polarization Method: Induced Polarization (IP) is a current stimulated electrical phenomenon observed as a delayed voltage response in earth material. The principles of IP method based on the electrical conduction, which in most rocks is essentially electrolytic, by transport of ions through interstitial water in pores. However, when a current is passed through a rock containing metallic minerals, the ionic conduction is hindered to a considerable extent by the mineral grains in which the current flow is electronic. This leads to an accumulation of ions at the interface between minerals and solution, resulting in a growth of electrochemical voltage at metallic grains surface. The process is similar to electrode polarization that occurs at the surface of metal electrodes dipped in an electrolyte. When the extremely applied current is switched off; the electrochemical voltage is dissipated, but does not drop to zero instantaneously. The decay in voltage is observed to vary with time, and can be measured as a fraction of the Voltage, (v) that existed when the current was flowing. The ratio v/V gives a measure of the concentration of a metallic mineral in the rock formation (Hallos, 1992).

IP measurement can be made using either DC or AC current. When measurements are made by sending DC pulses into the ground, the magnitude of IP is expected as V_t / V_o where V_t is the voltage remaining at a time t and V_o is the voltage that existed when the current

was flowing. The ratio V_t / V_o is expressed as a percent in terms of parameter called the Polarizability (ξ). This is defined as:

$$\xi = IP\% = 100 (V_t / V_o).$$

When an alternating current is put into the ground, the ratio of voltage to current measured becomes impedance rather than a resistance. The effective impedance and resistivity of the ground will depend on the frequency of the AC resistivity (ξf) and (ξf) are the measured apparent resistivities with the direction alternating currents, then the frequency effect (frequency domain) of IP can be expressed as:

$$PFE = 100 (\xi f - \xi f) / \xi f$$

In practice, F is usually in the range 0.05-0.5 Hz and F in the range 1-10Hz to remain in the non-inductive regions (Hallos, 1992). Another frequency-domain measure of IP is the Metal Factor (MF) which is defined as:

$$MF = 103 PFE \times \xi f$$

The constant multiplying factor of 10 is of no fundamental significance. In SI units MF has the dimensions siemens/m.

The field measurements were performed using Zonge Engineering GDP-16 multipurpose receiver and three phases ZMG-30 electrical generator with MXT-12 controller. The electrode configuration was a dipole-dipole array. Four IP lines were conducted in the study area (Fig. 5). Two-dimensional (pseudo-sections) apply in order to present the field measurement. The lateral position of the apparent values is plotted in relationship to where the electrodes were placed when that particular measurement was made. The distance of the plotted apparent value from measurement line is related to the space between the electrodes.

Field Results and Interpretation

Interpretation of Gravity Data: The object of interpretation is to establish possible relationships between the observed gravity anomalies and the different rock types occurring in the area under study, to demarcate different structural and tectonic elements. The interpretation process starts with a visual inspection of the shape and trend of relatively major anomalies. The Bouguer gravity map (Fig. 3) is characterized by a negative anomaly, of the order of -53 mGal to -58 mGal. The map shows that the gravity field maintains a general SE-NW trend (Al-Zoubi et al., 1999).

Interpretation of Magnetic Data: The process of interpretation of the ground magnetic survey began with a reduction of ground magnetic data to the pole of the total intensity magnetic map. This process had reduced (or at least minimized) the distortion effect of the magnetic pole. Careful inspection of this map (Fig. 4) reveals that the area under the study is characterized by numerous closures having high magnetic fields. These anomalies may reflect shallow causative bodies. The qualitative interpretation of the magnetic field allows us to trace the location of surface broken feature zones, fissure zones, dykes or lineaments. Deep and/or causative bodies (Al-Zoubi et al., 1999) may cause these zones.

Interpretation of HLEM Data: Knowledge of geology in the survey area was often rudimentary in interpreting HLEM data. The study area is located in a highly arid environment surrounded by hills at the east and west. The raw data for Tc-Rc separation equal 50 m are plotted as profiles at frequencies 1777, 888, 444, 222, and 111 Hz., respectively, which meant for the shallow and moderate depth of investigation (Figs. 6, 7, 8, 9, 10 and 11).

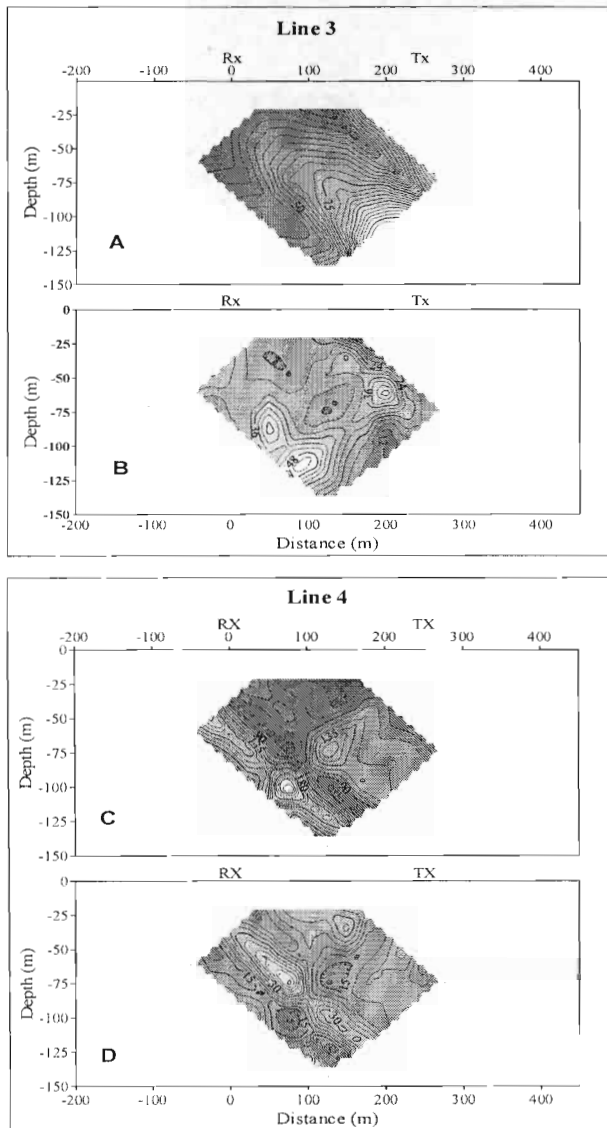


Fig. 13: Pseudo Section of the IP (Time domain) along the Lines 3 and 4 (for Location Fig. 5). Pseudo Sections (a and c) Represent Apparent Resistivity (ρ_a). Sections (b and d) Represent Metal Factor (MF)

In Figures 6 through 11 the data show low background response at the quadrature component at low frequencies (111 and 222 Hz). There is no visible anomaly on the quadrature components. Essentially zero mean background response was observed at the lowest frequency (111 and 222 Hz). At the higher frequencies (444, 888, and 1777 Hz), the mean background response becomes significant in both components. Higher background values were recorded on the quadrature component rather than on ten-phase component. The HLEM background response, which is increasing towards the northeast direction of the survey lines, indicates a change in the conductivity-

thickness product. This can be attributed to increasing thickness of the weathered layer from the west and southwest to east and northeast. This is in agreement with the geological data, where the rock sequences in the study area are dipping toward the NE.

The response of the altered zones as seen at high frequencies (1777 and 888 Hz; Figures 6 through 11) is characterized by two minima in the in-phase and quadrature components located at either side of the altered zone. This response can be mistakenly attributed to two parallel conductors under a uniform overburden. But the response is nothing other than the combination of the response of two ramps of the conductive zone. One when the thickness of the overburden layer goes from t to t' and other from t' to t , where, t is the thickness of the overburden layer and t' is the depth to the top of the conductive zone. The appearance of the maximum between the two minima is controlled by the width of the conductive zone and the coil separation.

From inspection of the anomaly curves, it is shown that the widths of the negative minimum parts of the in-phase and quadrature anomaly curves do not exceed the coil separation. This means that the width of the target is less than the coil separation. Thus, a maximum response in the in-phase and quadrature components appears over the conductive zone and the amplitude of the response increases with the size of the zone, as we would expect. This is in agreement with the work of Villegas-Garcia and West (1983). Accordingly, an interpretation is made assuming that a conducting half-plane induces the anomalies. By using a selected profile, 1777 Hz, the ratio of the negative minimum values on the in-phase and quadrature components, $Re2/Im2$, was found to be more than one. This indicates that a good conductive body is in question. Utilizing these criteria, conductive zones over the measured profiles was determined. These zones are shown as gray color Figures 6 through 11.

Interpretation of IP Measurements: The results of the Induced Polarization (IP) were presented in pseudo section (Fig. 12 (a, b, c and d)). The obtained results, which are explained on the pseudo cross sections, are described below:

Line 1, Figure 12 (a and b), runs 650 m long in N-S direction. The map shows that along this line two IP anomalies were obtained. The first one is located between point 50 m and 125 m (Fig. 12a). The relatively high metal factor (MF) values about 25 Siemens/m fit well with relatively low resistivity value (Fig. 12b), which reached about 50 Ohm-m. The second anomaly zone is located in the lower level and extends to point 200 and it has high resistivity value (more than 170 Ohm-m, Fig. 12a) and low metal factor (about 12 Siemens/m, Fig. 12b).

Line 2 is running about 650 m in NW-SE direction. It is shown in Fig. 12 (c and d). The obtained results show that the apparent resistivity reached a value of 94 Ohm-m (Fig. 12c), where The metal factor MF is very high, more than 110 Siemens/m (Fig. 12d). The MF value located between 50 m and 150 m. The apparent depth of this anomaly is about 110 m. it is worth mentioned here that the MF value first registered in Jordan and it needs more detailed study.

The pseudo section along line 3 is shown in Fig. 13 (a and b). This line is running along with electromagnetic line 009. Two anomalies were located, the first one has MF value of about 50 Siemens/m

(Fig. 13b) and it is located at apparent depth ranging from 90 m to 120 m. and the second anomaly located at a distance of about 200 m at the beginning of the line where, the MF value reached 48 Siemens/m. The apparent depth to the center of this anomaly is about 70 m.

Line 4 is located in the southern part of the study area with N-S direction (Fig. 5). The apparent resistivity and MF pseudo section are shown in Fig. 13 (c and d). Along this line one anomaly zone was recognized at about 50 m from the zero point. The MF value of this anomaly is reached 44 Siemens/m (Fig. 13d), where the apparent resistivity value is about 60 Ohm-m (Fig. 13c). It occurs at apparent depth of about 80 m. Below this anomaly a body of a high resistivity may occur which gives a value of more than 240 Ohm-m. Correlation between EM and IP results was made. It was found that the conductive zones over the study area align themselves along two trends, i.e., NNW and NW trends. Three trending zones have about 2.5 Km long trending NNW was also recognized. One zone trending NW were also observed in the southeastern corner (profile 004, Fig. 7). In addition, it was found that the dominant structures in the study area in the N-S and NW-SE trends.

Conclusion

A geophysical investigation was conducted at the central part of the Wadi Araba area, Jordan to delineate indicative of buried veins like bodies and to locate the mineralization zones. Gravity, magnetic, electromagnetic and induced polarization surveys were employed to achieve these objectives. Geophysical data obtained yield significantly alteration zones in the study area. It was found that the alteration zones in the study area align themselves along NNW-SSE and NW trends. This alteration zone probably host significant mineralization which needs further exploration and examination in order to determine the size, degree and extent of mineralization.

Acknowledgments: The authors indebted to the Natural Resources Authority of Jordan for supporting this work; special thanks for the General Director of the NRA Eng. Main Hiyari and Director of the Geology Department Eng. Darwish Jaser for their permission to publish this work.

References

Al-Zoubi, A., A. Batayneh; M. Hassounah; T. Talat and A. Abu Al Adas, 1999. Integrated geophysical studies for purposes of mineral exploration in Wadi Abu Khusheiba Area, Southwest Jordan. Natural Resources Authority, Amman, Jordan.

Bender, F., 1974. Geology of Jordan, Germany, Berlin, 196.

Betz, j., 1975. Test program report with additional comments on Max Min electromagnetic Sys. Markham, Apex Parametric Ltd., 34.

Betz, j., 1976. Considerations behind the making of a well-rounded exploration Sys. Markham, Apex Parametric Ltd., 14.

Biewinga, D., 1977. Electromagnetic depth sounding experiment. Geophysical Prospecting 25, 13-28.

Frei, L. and R. Freuned, 1990. Spatial and temporal relationships between two sets of strike-slip faults in southeastern Sinai. Tectonophysics, 180, 111-122.

Grant, F. and G. West, 1965. Interpretation theory in applied geophysics, McGraw-Hill, New York.

Hallof, G., 1992. Ground electrical methods in geophysical exploration. In practical geophysics II, 39-135.

Kaufmanns, A. and G. Keller, 1983. Frequency and transient sounding, Elsevier Publishing, Amsterdam.

Keiswetter, D. and I. Won, 1997. Multifrequency electromagnetic signature of the cloud chamber, Nevada test site. J. of Environmental and Eng. Geophysics 2, 99-103.

Keller, G. and F. Frischnecht, 1966. Electrical methods in geophysical prospecting, Pergamon Press, New York.

Lee, T., 1977. Estimation of depth to conductors by the use of electromagnetic transients. Geophysical Prospecting 25, 61-75.

Mart, Y. and A. David, 1987. Post Miocene rifting and diapirism in the northern Red Sea. Marine Geology 74, 173-190.

Mart, Y. and J. Hall, 1984. Structural trends in the northern Red Sea. J. Geophysical Research 89, 11352-11364.

Parasnis, D., 1966. Mining geophysics. Elsevier Publishing Company, Amsterdam.

Parasnis, D., 1971. Analysis of some multi-frequency, multi-separation electromagnetic surveys. Geophysical Prospecting 19, 163-179.

Patra, H. and K. Mallick, 1980. Geosounding Principle 2, Elsevier Scientific Publishing Company, New York.

Quennell, A., 1958. The structural and geomorphic evolution of the Dead Sea rift. J. Geology Society, London 114: 1-24.

Rabba, I., A. Masri; K. Moumani; A. Gharaibeh and K. Khrist, 1999. Geological map of Wadi Abu Khusheiba, scale 1: 10000, Natural Resources Authority, Jordan.

Rai, S. and S. Verma, 1982. Quantitative interpretation of Horizontal-Loop EM measurements using a permeable sphere model. Geophysical Prospecting 30, 486-500.

Spies, B., 1989. Depth of investigation in electromagnetic sounding methods. Geophysics 54, 872-888.

Villegas-Garcia, C. and G. West, 1983. Recognition of electromagnetic overburden anomalies with horizontal loop electromagnetic survey data. Geophysics 48, 42-51.

Warwick, B., N. Fawwaz; A. Mohammad; A. Hamzeh and S. Abdel Karim, 1996. Primary and secondary gold mineralization in Wadi Abu Khusheiba, southern Jordan. Natural Resources Authority, Jordan.

Won, I., 1980. A wide-band electromagnetic exploration method: some theoretical and experimental results. Geophysics 45, 928-940.